Food and Chemical Toxicology 125 (2019) 479–493

Contents lists available at ScienceDirect

Food and Chemical Toxicology

journal homepage: www.elsevier.com/locate/foodchemtox

Microbial metabolites of proanthocyanidins reduce chemical carcinogen-induced DNA damage in human lung epithelial and fetal hepatic cells *in vitro*

W.P.D. Wass Thilakarathna[a], H.P. Vasantha Rupasinghe[a,b,*]

[a] Department of Plant, Food, and Environmental Sciences, Faculty of Agriculture, Dalhousie University, Truro, Nova Scotia, Canada
[b] Department of Pathology, Faculty of Medicine, Dalhousie University, Halifax, Nova Scotia, Canada

ARTICLE INFO

Keywords:
Proanthocyanidin
DNA damage
Cancer
Microbial metabolites
Carcinogen
Antioxidant

ABSTRACT

Seven selected microbial metabolites of proanthocyanidins (MMP), 3-phenylpropionic, 4-hydroxyphenyl acetic, 3-(4-hydroxyphenyl) propionic, *p*-coumaric, benzoic acid, pyrogallol (PG), and pyrocatechol (PC) were evaluated for their ability to reduce chemical carcinogen-induced toxicity in human lung epithelial cells (BEAS-2B) and human fetal hepatic cells (WRL-68). Cells pre-treated with MMP were exposed to a known chemical carcinogen, 4-[(acetoxymethyl) nitrosamino]-1-(3-pyridyl)-1-butanone (NNKOAc) to assess MMP-mediated cytoprotection and reduction of DNA damage. PG in BEAS-2B and PC in WRL-68 cells mitigated the NNKOAc-induced cytotoxicity. Pre-incubation of PG depicted significant protection against NNKOAc-induced DNA damage in BEAS-2B cells. PC in WRL-68 cells showed similar activity. To understand the mechanisms of PG- and PC-mediated DNA damage reduction, the effect on DNA damage response (DDR) proteins, cellular reactive oxygen species (ROS), total antioxidant capacity (TAC), glutathione peroxidase (GPx), and caspase activity were studied. PG and PC alter the DDR and may promote ATR-Chk1 and ATM-Chk2 pathways, respectively. Cellular oxidative stress induced by NNKOAc was mitigated by PG and PC through enhanced GPx expression and TAC. PG and PC suppressed the activation of the extrinsic apoptotic pathway (caspase 3 and 8) provoked by NNKOAc. MMP are beneficial in chemoprevention by reducing cellular DNA damage.

1. Introduction

Cancer is a systemic disease characterized by genomic instability (Shen, 2011), contributed by inevitable daily exposure to carcinogens and metabolic processes primarily associated with oxidation (Jia et al., 2015). Lung and liver cancers are among the fatal types of cancers worldwide (Siegel et al., 2017). Tobacco smoking is a global issue identified as a significant risk factor for lung carcinogenesis (Molina et al., 2008). Cohort studies on the link between tobacco smoking and liver carcinoma reveal a positive and dose-responsive relationship (Pang et al., 2015). Polycyclic aromatic hydrocarbons and nicotine-derived nitrosamines are the two major groups of carcinogens in tobacco smoke (Pfeifer et al., 2002). Nicotine-derived nitrosamine, 4-(methylnitrosamino)-1-(3-pyridyl)-1-butanone (NNK) is a well-studied chemical carcinogen in cigarette smoke (Garcia-Canton et al., 2013).

Anticancer properties of plant-derived polyphenols and their synthetic derivatives are well documented (George et al., 2017; Sun et al., 2015; Vuong et al., 2014). Polyphenols are the largest group of phytochemicals and major contributor to antioxidant activity in the plant-based diet (Rupasinghe et al., 2013; Akinmoladun et al., 2007). Flavonoids, a sub-group of plant-derived polyphenols, are ubiquitously available in plants as pigments and further sub-classified as isoflavones, flavones, flavonols, flavanones, flavaols, and anthocyanidins (Tsao, 2010). PAC or the condensed tannins are the results of polymerization of flavanol monomers; predominantly catechins and epicatechins (Parmar and Rupasinghe, 2014; Si et al., 2006).

Despite the successful *in vitro* demonstrations of anticarcinogenic effects by complex polyphenols, their low bioavailability limits the clinical applications. Molecular weight and complexity determine the bioavailability of polyphenols (Thilakarathna and Rupasinghe, 2013).

Abbreviations: DDR, DNA damage response; DMSO, dimethyl sulfoxide; EDTA, ethylenediamine tetra-acetic acid; GPx, glutathione peroxidase; MMP, microbial metabolites of proanthocyanidins; MTS, (3-(4,5-dimethylthiazol-2-yl)-5-(3-carboxymethoxyphenyl)-2-(4-sulfophenyl)-2H-tetrazolium); NaOH, sodium hydroxide; NNK, 4-(methylnitrosamino)-1-(3-pyridyl)-1-butanone; NNKOAc, 4-[(acetoxymethyl) nitrosamino]-1-(3-pyridyl)-1-butanone; PAC, proanthocyanidins; PC, pyrocatechol; PG, pyrogallol; PMS, phenazine methosulphate; ROS, reactive oxygen species; TAC, total antioxidant capacity; γ-H2AX, phosphorylated histone protein H2AX

* Corresponding author. Department of Plant, Food, and Environmental Sciences, Faculty of Agriculture, Dalhousie University, Truro, Nova Scotia, Canada.
E-mail address: vrupasinghe@dal.ca (H.P.V. Rupasinghe).

https://doi.org/10.1016/j.fct.2019.02.010
Received 5 August 2018; Received in revised form 12 January 2019; Accepted 4 February 2019
Available online 05 February 2019
0278-6915/ © 2019 Elsevier Ltd. All rights reserved.

Dietary PAC with more than four monomers are not absorbed by small intestine but catabolized by colonic microbiota into phenylvalero lactones and phenolic acids (Ou and Gu, 2014; Thilakarathna et al., 2018).

Anticancer properties of these metabolites are still not well understood. Therefore, in this study potential of selected MMP in the reduction of cancer risk is investigated using chemically-induced DNA damage mitigation. Seven previously identified MMP; 3-phenylpropionic acid, 3-(4-hydroxyphenyl)propionic acid, 4-hydroxyphenyl acetic acid, benzoic acid (Deprez et al., 2000), *p*-coumaric acid (Li et al., 2013), PG and PC (Tabasco et al., 2011) were assessed for their capacity in reduction of carcinogen-induced DNA damage. The experimental model is developed by considering the positive association of tobacco smoking with lung and liver cancers. Investigation of anticancer properties of MMP is useful in the discovery of cancer preventive drugs and development of synbiotic food and nutraceutical products potent in cancer chemoprevention.

2. Materials and methods

2.1. Chemicals and reagents

3-Phenylpropionic acid (W288918), 4-hydroxyphenyl acetic acid (H50004), 3-(4-hydroxyphenyl)propionic acid (H52406), *p*-coumaric acid (C9008), benzoic acid (242381), PG (254002), and PC (C9510) were purchased from Sigma-Aldrich (Oakville, ON, Canada). Bronchial Epithelial Basal Medium (BEBM) and Bronchial Epithelial Growth Medium (BEGM) kit were purchased from Lonza (Walkersville, MD, USA). Minimum Essential Medium Eagle (MEME), fetal bovine serum (FBS), penicillin-streptomycin, bovine collagen type-1, fibronectin (from human plasma), L-glutamine, bovine serum albumin (BSA), dimethyl sulfoxide (DMSO), phosphate buffered saline (PBS), trypan blue stain, phenazine methosulphate (PMS) were purchased from Sigma-Aldrich (Oakville, ON, Canada). All chemicals and reagents were of research grade and suitable in cell culture experiments where applicable.

2.2. Cell lines and culture conditions

Two normal human cell lines were used in this study. Lung bronchial epithelial cells/BEAS-2B (ATCC® CRL-9609™) and fetal hepatic cells/WRL-68 (ATCC® CL-48™) were purchased from American Type Culture Collection (Manassas, VA, USA). BEAS-2B cells were cultured in BEGM prepared by the addition of BEGM kit into BEBM. Gentamycin-amphotericin B mix provided with the BEGM kit was replaced with 100 U/ml penicillin, and 100 μg/mL streptomycin (as per the instructions by ATCC®). Culture flasks and well plates were pre-coated overnight with 0.01 mg/mL fibronectin, 0.03 mg mL bovine collagen type-1 and 0.01 mg/mL BSA prior to the seeding of cells. WRL-68 cells were cultured in MEME supplemented with 10% FBS, 4 mM L-glutamine, 100 U/ml penicillin and 100 μg/mL streptomycin. Cell cultures were maintained at 37 °C and 5% CO_2 in a humidified incubator (3074, VWR International, Edmonton, AB, Canada) and sub-cultured before reaching confluence.

2.3. MTS cell viability assay for evaluation of concentration-dependent MMP cytotoxicity

Concentration-dependant cytotoxicity of the MMP was evaluated using CellTiter 96® AQ_{ueous} MTS reagent powder (Promega, Madison, WI, USA) to identify sensible MMP concentrations for future experiments. Cells were seeded in 96-well plates at a density of 6000 cells/well and incubated overnight at 37 °C. Following incubation, cells were treated with 10 concentrations (0.1, 1, 10, 25, 50, 75, 100, 250, 500, and 1000 μM) of each MMP separately, and incubated for 24 h at 37 °C. Treated cells were exposed to the MTS/PMS solution (MTS, 333 μg/mL; PMS, 25 μM of final concentration) and incubated for 3 h at 37 °C. After incubation absorbance was measured at 490 nm using the Infinite® M200 PRO multimode microplate reader (Tecan Trading AG, Mannedorf, Switzerland).

2.4. 7-AAD stained flow cytometry for evaluation of concentration-dependant MMP cytotoxicity

Cells were seeded in 6-well culture plates at a density of 2×10^5 cells/well and incubated overnight at 37 °C. Cells were treated with 10 concentrations (0.1, 1, 10, 25, 50, 75, 100, 250, 500, and 1000 μM) of each MMP separately, and incubated at 37 °C for 24 h. After the 24 h incubation period, culture media in wells were collected into separate tubes to include potential dead cells in the assay. Adhered cells were harvested by using TrypLE express (1 mL/well, incubated for 5 min at 37 °C) and pooled with the collected culture media. Samples were centrifuged at 500 × *g* for 5 min, and the supernatant was discarded. The cell pellet was suspended in 1 mL of PBS and stained with 7-AAD stain (eBioscience™ 7-AAD viability staining solution, ThermoFisher Scientific, Waltham, MA, USA) in the dark. Samples were analyzed by fluorescence-activated cell sorting (FACS) under the FL-3 filter and data were processed using FCS Express 6 plus Research Edition software.

2.5. Amplex® Red assay to investigate H_2O_2 production by MMP in cell culture medium

Cytotoxicity depicted by PG and PC can be caused by the production of H_2O_2 in the culture medium (Kelts et al. 2015). Potential of PG and PC for H_2O_2 production in culture medium (cell-free system) was investigated using Amplex® Red assay kit (ThermoFisher Scientific, Waltham, MA, USA). Standards of H_2O_2 (up to 1000 μM) and the MMP treatments used in MTS assay were prepared (in 2 × concentrations) in phenol red-free complete growth medium and pipetted (100 μL) into 96-well plates. The Amplex® Red master mix was made by adding Amplex® Red solution (final concentration; 25 μM) and horseradish peroxidase (final concentration; 0.005 U/mL) into phenol red-free growth medium. Standards and the MMP treatment aliquots in 96-well plates were mixed with 100 μL of master mix and incubated in the dark at 37 °C for 2 h. After incubation absorbance of the wells was measured at 570 nm using the Infinite® M200 PRO multimode microplate reader (Tecan Trading AG, Mannedorf, Switzerland). H_2O_2 production by each MMP treatment was calculated by creating the H_2O_2 standard curve.

2.6. Oregon Green® assay to measure MMP promoted cell proliferation

Lower concentrations of PG and PC exhibited considerably high % cell viability for BEAS-2B cells in MTS cell viability assay. High % cell viability may be due to the promotion of cell proliferation. First, the cells were synced-up by incubating in serum-free medium for 24 h to bring all cells to the same phase of the cell cycle. Following synchronization, cells were seeded in 6-well plates (at 1×10^5 cells/well) with complete growth medium and incubated overnight at 37 °C. Oregon Green® 488 (Carboxy DFFDA-SE) was purchased from ThermoFisher Scientific (Waltham, MA, USA). Oregon Green® stock solution was prepared by addition of 16.80 μL of DMSO to a vial (contained 50 μg). The stock solution was diluted in serum-free culture medium (0.25 μL/mL) to produce a working solution. Wells were washed with warm 1 × PBS and added with 1 mL of Oregon Green® working solution prior to incubation at 37 °C in the dark for 45 min. After incubation, wells were washed with warm complete growth media and cells were allowed to recover in the dark for 2 h at 37 °C in complete growth media (2 mL/well). After the cell recovery period cells in control wells (non-proliferative controls) were harvested and fixed in 0.5 mL of 1% paraformaldehyde in 1 × PBS. Non-controls of BEAS-2B cells were treated with 1, 10, and 25 μM concentrations of PG and PC while WRL-68 cells were treated with 10, 25, and 50 μM concentrations of the same MMP.

After 72 h of MMP treatment cells were harvested and fixed in 1% paraformaldehyde in 1 × PBS. Non-proliferative controls and treated cells were stored in the dark soon after fixation. Finally, the prepared samples were analyzed by FACS and data were processed using FCS Express 6 plus Research Edition software.

2.7. MTS assay to study MMP-mediated cytoprotection against NNKOAc

MTS protocol identical to section 2.3 was followed with an additional treatment step. Based on MTS results for evaluation of concentration-dependant cytotoxicity of MMP, cells were treated with 4 concentrations (10, 25, 50, and 250 μM) of each MMP separately for 24 h and challenged for cytotoxicity by NNKOAc (300 μM, 4 h). After incubation with NNKOAc % cell viability was measured using the MTS assay.

2.8. PG and PC-mediated protection against NNKOAc induced cellular DNA damage

The degree of protection by MMP in NNKOAc-induced DNA damage was measured by the H2AX immunofluorescence assay. As per MTS assay test results from the study of MMP-mediated cytoprotection against NNKOAc, 10 and 25 μM concentrations of PG were selected as the treatments for BEAS-2B cells. For WRL-68 cells, 25 and 50 μM concentrations of PC were the selected treatments. Cells were seeded in 6-well plates (2×10^5 cells/well) included with 95% ethanol sterilized glass coverslips. Cells were allowed to adhere overnight on the coverslip surfaces and treated with PG and PC for 24 h. Following PG and PC treatments cellular DNA damage was induced by using NNKOAc (300 μM for 4 h). Cells were allowed to recover for 4 h to facilitate maximum phosphorylation at DNA damage sites and washed with 2 mL of PBS to reduce background staining. Cells were fixed onto coverslips by adding 2 mL of 3.7% formaldehyde and incubating in the dark for 20 min at room temperature (RT). Fixed cells were permeabilized by exposing to 0.5% Triton X-100 in PBS for 15 min at RT. Triton X-100 was thoroughly removed from wells by washing with PBS. Cells were blocked by transferring coverslips onto drops (55 μL) of 4% BSA in PBS on parafilm in humidifying chambers and incubating at RT for 20 min. Incubation with primary antibody (anti-phospho-histone H2A.X (Ser139), Life Technologies, Eugene, OR, USA) was done similarly by transferring coverslips onto drops (55 μL) of primary antibody diluted 1:250 in 4% blocking solution for 1 h in the dark at RT. Coverslips were transferred back into respective wells and excess of primary antibody was washed-off using PBS. Cells were incubated with secondary antibody (Alexa fluorophore® 594 donkey anti-mouse IgG, Life Technologies, Eugene, OR, USA) diluted 1:500 in 4% BSA blocking solution by transferring onto drops of secondary antibody in humidifying chambers (at RT for 45 min in the dark). Excess of secondary antibody was washed off similar to washing after incubation with the primary antibody. Coverslips were wet-mounted on glass slides using mounting media containing DAPI (Vector Laboratories Inc., Burlingame, CA, USA). All slides were imaged by fluorescence microscopy, and number of phosphorylated H2AX foci were counted using ImageJ (Version 1.51j8) software (Schneider et al., 2012).

2.9. Effect of PG and PC in NNKOAc-induced DDR mechanisms

The influence of PG and PC on cellular DDR mechanisms was studied by using the western blot. Cellular abundance of DDR proteins: *p*-ATM (Ser1981), *p*-ATR (Ser428), *p*-p53 (Ser15), and γ-H2AX (Ser139) was measured. Activation of cell cycle checkpoint kinases Chk1 (Ser345) and Chk2 (Thr68) was monitored by measuring the levels of *p*-Chk1 and *p*-Chk2. Levels of *β*-actin were measured for each treatment as the housekeeping protein to eventually normalize the expressions of the measured proteins (George and Rupasinghe, 2017). All antibodies (DNA damage antibody sampler kit) were purchased from Cell Signaling Technology® (Danvers, MA, USA). BEAS-2B cells were treated with 10 and 25 μM concentrations of PG for 24 h. WRL-68 cells were treated with 25 and 50 μM concentrations of PC for 24 h. PG and PC treated cells were exposed to 300 μM NNKOAc for 4 h to induce DNA damage. Each experimental model consisted of a DMSO control, NNKOAc control, and controls from respective concentrations of PG and PC. Radio-immunoprecipitation assay (RIPA) buffer was prepared by mixing 50 mM Tris HCl, 150 mM NaCl, 1% Triton X-100, 0.5% sodium deoxycholate, 1 mM EDTA, and 10 mM NaF. Protease inhibitor cocktail (Sigma-Aldrich, Oakville, ON, Canada) was added to the RIPA buffer (10 μL/1 mL of RIPA buffer) prior to use. After the treatments, cells were harvested, and the proteins were extracted by using RIPA buffer. The protein contents of extracted protein samples were estimated by Pierce™ Coomassie (Bradford) protein assay kit (ThermoScientific, Rockford, IL, USA).

Extracted proteins were denatured by using Blue Loading Buffer Pack by New England BioLabs™ Inc (Ipswich, MA, USA). Protein samples were loaded (20 μg/well) into the wells of precast SDS-gel cassettes (Mini-PROTEAN® TGX Stain-Free™ Gels, Bio-Rad Laboratories Inc., Hercules, CA, USA) and subjected to electrophoresis using BIO-RAD Mini PROTEAN® Tetra Cell gel electrophoresis unit (90 min at 80 V and 400 mA). Protein separated on SDS-gels by electrophoresis were transferred onto polyvinylidene difluoride (PVDF) membranes (ThermoScientific, Rockford, IL, USA) by using BIO-RAD Trans-Blot® Turbo™ system (Hercules, CA, USA). PVDF membranes were blocked with blocking solution; non-fat milk powder (5% w/v) in 1×Tris-buffered saline (TBST) (Cell Signaling Technology, Danvers, MA, USA), for 1 h at RT. Blocked PVDF membranes were incubated with 10 mL of primary antibody solutions (1:1000 v/v in 5% BSA) at 4 °C overnight and washed with 1×TBST before reprobing with secondary antibodies (1:5000 in 5% non-fat milk powder in 1×TBST) for 1 h at RT. The membranes were washed with 1×TBST and developed by using enhanced chemiluminescence (ECL) based Clarity™ and Clarity Max™ Western ECL Substrates Kit (Bio-Rad Laboratories Inc., Hercules, CA, USA) to be imaged by BIO-RAD Chemidoc MP™ imaging system (Universal hood III, Hercules, CA, USA). Membranes were imaged in signal accumulation mode and analyzed for band intensities using ImageJ (version 1.51j8) software (Schneider et al., 2012). Protein levels were normalized compared to the level of *β*-actin, and the results were expressed in relative protein levels compared to the DMSO control. Protein levels were compared with the NNKOAc control where DMSO control failed to generate a measurable band.

2.10. Effect of PG and PC on NNKOAc-induced cellular ROS production

The ability of NNK to promote cellular ROS production in BEAS-2B cells is previously reported (Demizu et al., 2008). The effect of PG and PC on NNKOAc-mediated ROS production in BEAS-2B and WRL-68 cells were studied by the DCFDA/H2DCFDA – Cellular Reactive Oxygen Species Detection Assay Kit (Abcam, Toronto, ON, Canada). Cells were seeded in dark clear bottom 96-well culture plates at a density of 2.5×10^4 cells/well and incubated overnight at 37 °C. BEAS-2B and WRL-68 cells were treated with 10 and 25 μM PG and 25 and 50 μM PC respectively for 24 h at 37 °C. Cells were gently washed with the 1×buffer (100 μL) provided with the assay kit and stained with 25 μM DCFDA (in 1×buffer) for 45 min at 37 °C. DCFDA staining solution was removed, and the cells were washed again with 100 μL of the 1× buffer. ROS production was promoted by treating the cells with NNKOAc (300 μM) for 4 h at 37 °C. Excitation/emission for the wells was measured at 485/535 nm by Infinite® M200 PRO multimode microplate reader (Tecan Trading AG, Mannedorf, Switzerland). Results were expressed in fold increment or decrement compared to the control.

2.11. Effect of PG and PC on TAC of NNKOAc-treated BEAS-2B and WRL-68 cells

Alteration of the TAC by PG and PC in NNKOAc-treated cells was investigated by a commercially available antioxidant assay kit (Cayman Chemical Company, Ann Arbor, MI, USA) measuring the ability of cell lysates to prevent the oxidation of ABTS® by metmyoglobin. Cells were seeded in 6-well culture plates at a density of 2×10^5 cells/well and incubated overnight at 37 °C. BEAS-2B and WRL-68 were treated with 10 and 25 μM of PG and 25 and 50 μM of PC respectively, for 24 h at 37 °C. Cells were treated with NNKOAc (300 μM) for 4 h at 37 °C to challenge cellular antioxidant levels. Cells were harvested by using a rubber policeman and centrifuged at 1000× g for 10 min (4 °C). The resulting cell pellet was homogenized in cold buffer (5 mM potassium phosphate, 0.9% sodium chloride and 0.1% glucose, final pH 7.4) and centrifuged at 10,000× g for 15 min (4 °C). The supernatant was collected and pipetted (10 μL) into 96-well plate along with Trolox standards (0–0.33 mM), and mixed with metmyoglobin (10 μL) and chromogen (150 μL) provided with the assay kit. The reaction was initiated by addition of hydrogen peroxide (40 μL) and shaking the 96-well plates for 5 min at RT. Absorbance for each well was measured at 750 nm by Infinite® M200 PRO multimode microplate reader (Tecan Trading AG, Switzerland). Results were normalized to the protein concentrations of cell lysates (Pierce™ Coomassie protein assay kit, ThermoScientific, Rockford, IL, USA) and expressed in fold increment or decrement compared to the control.

2.12. Effect of PG and PC on GPx activity of NNKOAc-treated BEAS-2B and WRL-68 cells

The effect of PG and PC on cellular GPx activity was studied by using Glutathione Peroxidase Assay Kit purchased from Cayman Chemical Company (Ann Arbor, MI, USA). Cells were seeded in 6-well culture plates at a density of 2×10^5 cells/well and incubated overnight at 37 °C. BEAS-2B and WRL-68 were treated with 10 and 25 μM of PG, and 25 and 50 μM of PC, respectively, for 24 h at 37 °C. Cells were treated with NNKOAc (300 μM) for 4 h at 37 °C and harvested by using a rubber policeman. Cells were centrifuged at 1000× g for 10 min (4 °C), and the resulting cell pellet was homogenized in cold buffer (50 mM Tris-HCl, 5 mM EDTA, 1 mM DTT, final pH 7.5). The homogenized cell sample were centrifuged at 10,000× g for 15 min (4 °C), and the supernatant was collected to measure GPx activity. Collected supernatant was pipetted (20 μL) into 96-well plate and mixed with assay buffer (100 μL) and co-substrate mixture (50 μL) provided with the assay kit. The reaction was initiated by adding cumene hydroperoxide (20 μL) to each well. Absorbance for each well was measured at 340 nm over a period of 10 min, (enzyme kinetic mode) using Infinite® M200 PRO multimode microplate reader (Tecan Trading AG, Mannedorf, Switzerland). Results were normalized to the protein concentrations of cell lysates (Pierce™ Coomassie protein assay kit, ThermoScientific, Rockford, IL, USA) and expressed in fold increment or decrement compared to the control.

2.13. Effect of PG and PC on caspase activity of NNKOAc treated BEAS-2B and WRL-68 cells

The effect of PG and PC on cellular caspase-3, 8, and 9 activities was studied by caspase 3, caspase 8 and caspase 9 multiplex activity assay kit (Abcam, Toronto, ON, Canada). Cells were seeded in black clear bottom 96-well plates at a density of 1×10^4 cells/well and incubated overnight at 37 °C. BEAS-2B and WRL-68 cells were treated with PG (10 and 25 μM) and PC (25 and 50 μM) respectively and incubated for 24 h at 37 °C. Cells were treated with NNKOAc (300 μM) for 4 h at 37 °C to induce apoptosis. Each well was added with 100 μL of caspase assay loading solution with substrates for caspase 3, 8, and 9 (50 μL of each substrate in 10 mL of assay buffer) and incubated in the dark for 1 h at RT. Fluorescence of each well was measured (excitation/emission) at 535/620 nm (red), 490/525 nm (green), and 370/450 nm (blue) to evaluate the activities of caspase 3, 8, and 9, respectively (Infinite® M200 PRO multimode microplate reader, Tecan Trading AG, Mannedorf, Switzerland). Results were expressed in fold increment or decrement compared to the control.

2.14. Statistical analysis

Data were analyzed using Minitab statistical software (version 18). Results were expressed as the mean ± standard deviation of three individual experiments performed in triplicates. Means were compared by analysis of variance/ANOVA (99% confidence level) with Tukey's multiple mean comparison (95% confidence level).

3. Results

3.1. Concentration-dependent cytotoxicity of MMP

To understand the concentration-depended cytotoxicity of the selected MMP on BEAS-2B and WRL-68 cells, the MTS assay and 7-AAD stained-flow cytometry were performed (Fig. 1). Four of the MMP, 3-phenylpropionic, 4-hydroxyphenyl acetic, 3-(4-hydroxyphenyl) propionic and *p*-coumaric acid were not cytotoxic (over 80% cell viability) to the cell lines within the tested concentration range of 0.1–1000 μM (Supplementary Fig. 1). Benzoic acid showed cytotoxicity in BEAS-2B cells at the highest 1000 μM concentration (< 60% cell viability) with no signs of cytotoxicity in WRL-68 cells (over 80% cell viability). However, cytotoxicity by PG and PC was concentration-dependent in both cell lines (Fig. 1). Interestingly, as per the MTS test results, PG and PC promoted the cell viability in BEAS-2B cells at 1, 10, and 25 μM concentrations. However, 7-AAD flow cytometry results showed no evidence of promoted cell viability by PG in the BEAS-2B cells. Based on these results 10, 25, 50, and 250 μM concentrations were selected for the evaluation of the potential of the seven MMP in cytoprotection against NNKOAc.

3.2. PG and PC-mediated H_2O_2 production in cell culture media

Experimental results on cytotoxicity of phenolics *in vitro* are often misguided by the production of H_2O_2 and other reactive oxygen species (ROS) in the culture media (Lapidot et al., 2002). Potential of PG and PC for production of H_2O_2 in cell-free BEGM and complete MEME media was evaluated by Amplex® Red assay, to ensure the selected concentrations cause no misguided results in this study. PG and PC produced H_2O_2 in a concentration-dependent manner in both BEGM and complete MEME media (Fig. 2), especially at higher concentrations (≥ 250 μM). However, 250 μM concentration was included for the experimentation of MMP-mediated cytoprotection, as the other MMP except PG and PC exhibited no cytotoxicity at 250 μM.

3.3. Effect of PG and PC on cell proliferation

To understand whether the observed promoted cell viability by certain concentrations of PG and PC is related to increased cell proliferation, Oregon Green® assay was conducted. In contrast to the MTS assay results, PG limited the proliferation of BEAS-2B and WRL-68 cells in a concentration-dependent manner (Fig. 3 A and C). PC showed similar activity to PG in BEAS-2B cells (Fig. 3 B). However, PC did not impact the proliferation of WRL-68 cells (Fig. 3 D).

3.4. Identification of MMP effective against NNKOAc-induced cytotoxicity

The MTS assay was used to investigate the potential of MMP in the mitigation of NNKOAc-induced cytotoxicity. Among the tested MMP, only PG and PC exhibited the ability to protect BEAS-2B and WRL-

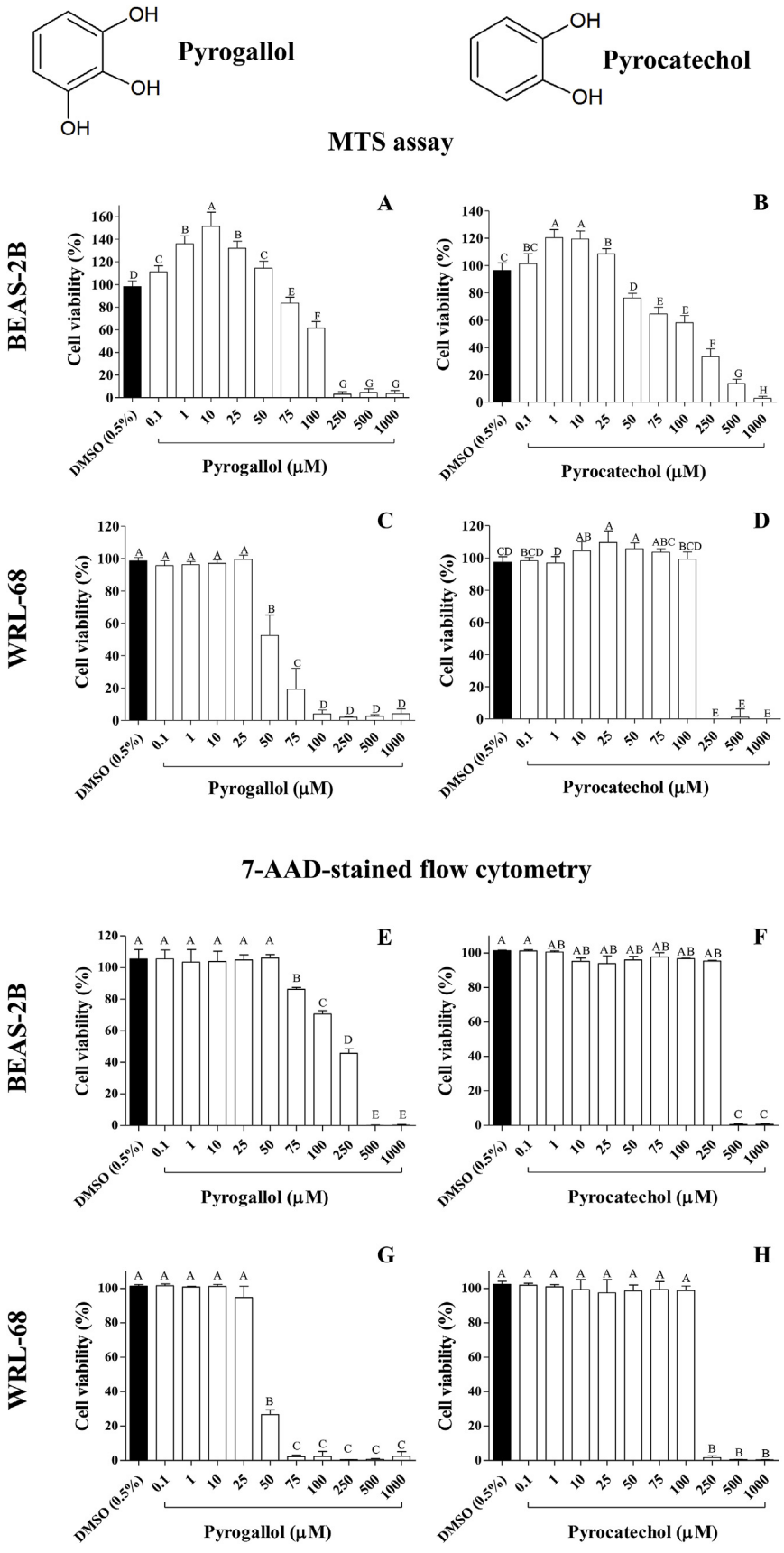

Fig. 1. Cytotoxicity of pyrogallol and pyrocatechol in BEAS-2B and WRL-68 cells. Cells were treated with pyrogallol or pyrocatechol for 24 h and measured for % cell viability using the MTS assay and 7-AAD stained flow cytometry. Concentration-dependent cytotoxicity of pyrogallol and pyrocatechol in BEAS-2B (A, B, E, F) and WRL-68 cells (C, D, G, H). Results were presented as mean ± SD of three independent experiments. Means that do not share a similar letter are significantly different ($p \leq 0.01$).

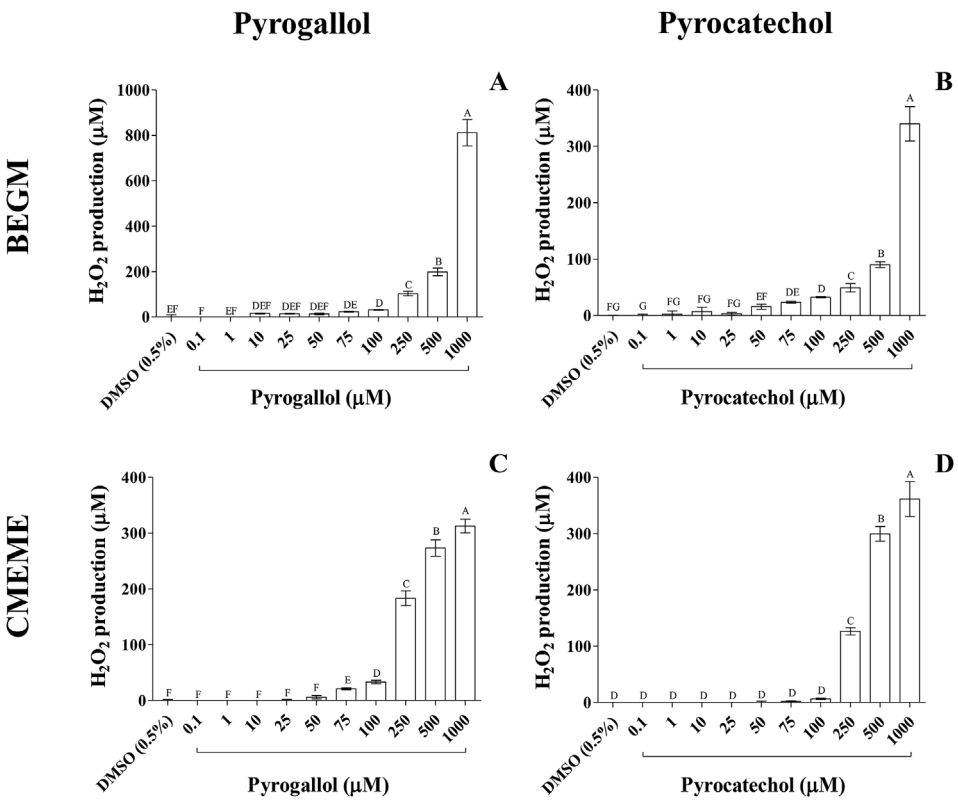

Fig. 2. Pyrogallol and pyrocatechol-mediated H_2O_2 production in BEGM (A, B) and CMEME (C, D) media. Treatment concentrations (0.1–1000 μM) of pyrogallol and pyrocatechol were prepared in cell-free culture media, and H_2O_2 production was measured by Amplex® Red assay (2 h of incubation at 37 °C). Results were presented as mean ± SD of three independent experiments. Means that do not share a similar letter are significantly different ($p \leq 0.01$).

68 cells against NNKOAc-induced cytotoxicity in a cell-type dependent manner (Fig. 4). PG depicted significant cytoprotection at 10, 25 and 50 μM concentrations in BEAS-2B cells, while these concentrations were not effective in the WRL-68 cells. PC showed the cytoprotection in both cell lines; however, its cytoprotection in WRL-68 cells was very distinctive at 25–50 μM concentrations. The PC-mediated cytoprotection in BEAS-2B cells was less than 50% at the tested concentrations and therefore was not included in further experimentation. Based on these observations, 10 and 25 μM concentrations of PG were selected to investigate their ability in the reduction of NNKOAc-induced DNA damage in BEAS-2B cells. Similarly, 25 and 50 μM concentrations of PC were selected for the WRL-68 cells.

3.5. PG and PC reduce NNKOAc-induced cellular DNA damage

Potential of PG and PC in the reduction of NNKOAc-induced DNA damage was assessed by using the γ-H2AX immunofluorescence assay. The γ-H2AX assay specifically detects double-strand breaks in cellular DNA through detecting DNA damage induced repair protein phosphorylated histone H2AX at the damage site (Ivashkevich et al., 2012). These damage sites appear in fluorescence microscopic images as red dots within the DAPI-stained blue color nuclei (Fig. 5). The DNA damage caused by NNKOAc was extremely intense in both cell lines, but the tested compounds also showed some induction of γ-H2AX. DNA damage initiated by NNKOAc in BEAS-2B cells pre-exposed to PG was significantly reduced ($p \leq 0.01$) at 10 and 25 μM concentrations (Fig. 5 A). Similarly, PC reduced the NNKOAc-induced DNA damage in WRL-68 cells in a concentration-dependent manner (Fig. 5 B).

3.6. PG and PC alters the abundance of DDR proteins

PG in BEAS-2B cells and PC in WRL-68 cells significantly altered the abundance of DDR proteins (Fig. 6). Treatment with NNKOAc upregulated the expression of all tested DDR proteins in BEAS-2B and WRL-68 cells. In BEAS-2B cells exposed to NNKOAc, 10 μM PG downregulated the expression of *p*-ATM compared to the NNKOAc control (Fig. 6 A-a). PG upregulated the expression of *p*-ATR in NNKOAc treated BEAS-2B cells at both 10 and 25 μM concentrations compared to the NNKOAc control (Fig. 6 A-b). Expression of *p*-Chk1, *p*-Chk2, *p*-p53, and γ-H2AX was downregulated in NNKOAc treated BEAS-2B cells by both 10 and 25 μM concentration of PG (Fig. 6 A-c,d.e,f). Downregulation of *p*-Chk1 and γ-H2AX was dependant on the PG concentration.

In contrast to PG in BEAS-2B cells, PC upregulated the expression of *p*-ATM, *p*-p53, and γ-H2AX in WRL-68 cells exposed to NNKOAc (Fig. 6 B-g,k,l). PC enhanced the expression of *p*-ATM in NNKOAc treated WRL-68 cells at both 25 and 50 μM concentration. The levels of *p*-p53 and γ-H2AX in NNKOAc treated WRL-68 cells were only improved at 50 and 25 μM concentrations of PC, respectively. Furthermore, in contrast to the influence of PG in BEAS-2B cells PC (25 μM) restricted the expression of *p*-ATR in WRL-68 cells exposed to NNKOAc (Fig. 6 B-h). PC downregulated *p*-Chk1, and *p*-Chk2 expression in NNKOAc treated WRL-68 cells at both 25 and 50 μM concentrations. Downregulation of *p*-Chk2 by PC was concentration-dependant.

3.7. PG and PC reduce the cellular oxidative stress

Chemical carcinogens such as NNK are known for elevating the cellular ROS level (Demizu et al., 2008), and the presence of ROS in excessive level significantly promote the cellular DNA damage (Cadet and Wagner, 2013). Thus, we studied the potential of PG and PC to affect cellular ROS levels, TAC, and antioxidant enzyme GPx, in cells exposed to NNKOAc. Significantly high levels of ROS were detected in BEAS-2B and WRL-68 cells exposed to NNKOAc (Fig. 7 A and B). PG in BEAS-2B cells and PC in WRL-68 cells reduced the cellular ROS levels induced by NNKOAc. PG and PC alone did not promote ROS when compared to the DMSO control. The TAC of BEAS-2B cells exposed to NNKOAc was significantly suppressed (Fig. 7 C). Such suppression of TAC was not observed for WRL-68 cells (Fig. 7 D). PG in BEAS-2B cells and PC in WRL-68 cells significantly elevated the cellular TAC with

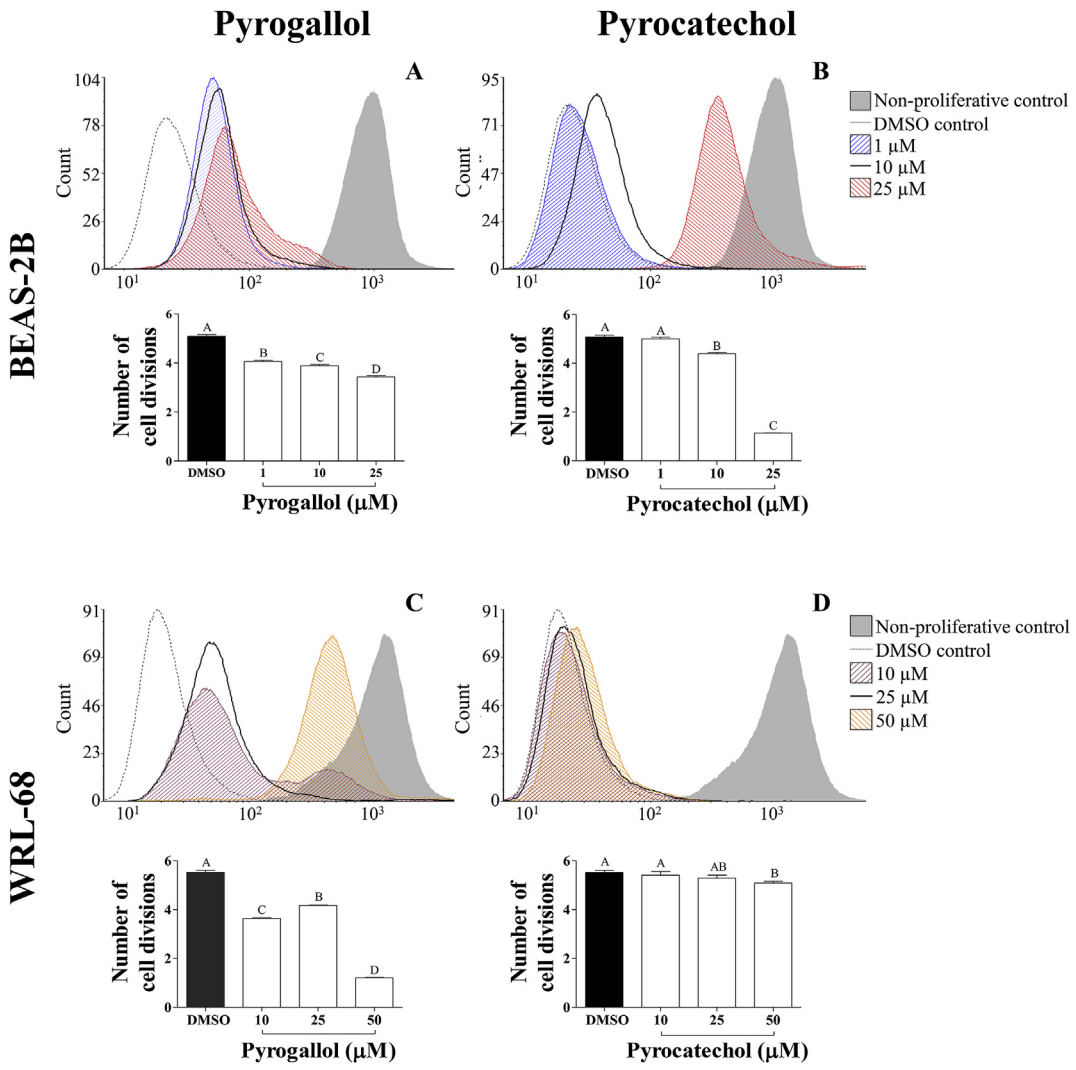

Fig. 3. Effect of pyrogallol and pyrocatechol on the proliferation of BEAS-2B and WRL-68 cells. The cells were treated with low concentrations (10, 25, and 50 μM) of pyrogallol and pyrocatechol for 72 h and assessed for effect on cell proliferation by Oregon® green-flow cytometry assay. Each experiment was repeated for three times to ensure the reproducibility of data. Data were processed and plotted using FCS Express 6 plus Research Edition software. Means that do not share a similar letter are significantly different ($p \leq 0.01$). (For interpretation of the references to color in this figure legend, the reader is referred to the Web version of this article.)

increasing concentration. When exposed to NNKOAc, cellular TAC promoted by PG and PC was significantly reduced, yet sustaining TAC level over PG and PC untreated cells. Exposure of BEAS-2B cells to NNKOAc substantially increased the GPx expression (Fig. 7 E). Such increment was not observed (instead of a reduction) for the WRL-68 cells (Fig. 7 F). PG increased the GPx activity in BEAS-2B cells with increasing concentration. In contrast, PC limited the GPx activity in WRL-68 cells. PG and PC significantly increased the GPx activity in BEAS-2B and WRL-68 cells respectively, when exposed to NNKOAc.

3.8. PG and PC reduce cellular caspase-3 and 8 expression

The crosstalk between DNA damage and cell apoptosis (hence activation of caspases) is of great importance in determining the cancer initiation and therapeutic responses (Nowsheen and Yang, 2012). Thus, the expression of key caspases (3, 8, and 9) important for intrinsic and extrinsic apoptotic pathways was studied for the cells treated with PG and PC, and exposed to NNKOAc. Caspase-3 and 8 activities of both cell lines were significantly increased when exposed to NNKOAc (Fig. 8). Caspase-3 and 8 expressions promoted by NNKOAc exposure were suppressed by the pre-exposure of PG and PC in BEAS-2B and WRL-68 cells, respectively. Interestingly, both PG and PC were able to suppress the caspase-3 and 8 expressions even lower than of DMSO control. PG in BEAS-2B and PC in WRL-68 cells not exposed to NNKOAc reduced the caspase-3 and 8 expressions compared to the DMSO control. Caspase-9 expression was affected in either cell line by neither NNKOAc exposure nor PG and PC treatments.

4. Discussion

The experimental model of this study was developed by considering the well-studied positive relationship between tobacco smoking and lung carcinogenesis, to test the potential of MMP in the prevention of DNA damage *in vitro*. BEAS-2B cells pre-exposed to MMP were challenged for cytotoxicity and genotoxicity induced by NNKOAc (Fig. 9). Chemical carcinogen NNKOAc mimics the carcinogenicity of NNK, a major nicotine-derived carcinogen in cigarette smoke. Cellular cytochrome P450 activity is essential in the metabolism of NNK to generate secondary metabolites capable in carcinogenesis (Garcia-Canton et al., 2013). Cyto and genotoxicity of NNK can be limited in BEAS-2B cells due to low cytochrome activity (Garcia-Canton et al., 2013). Carcinogen NNKOAc requires no cytochrome P450 activity for cellular

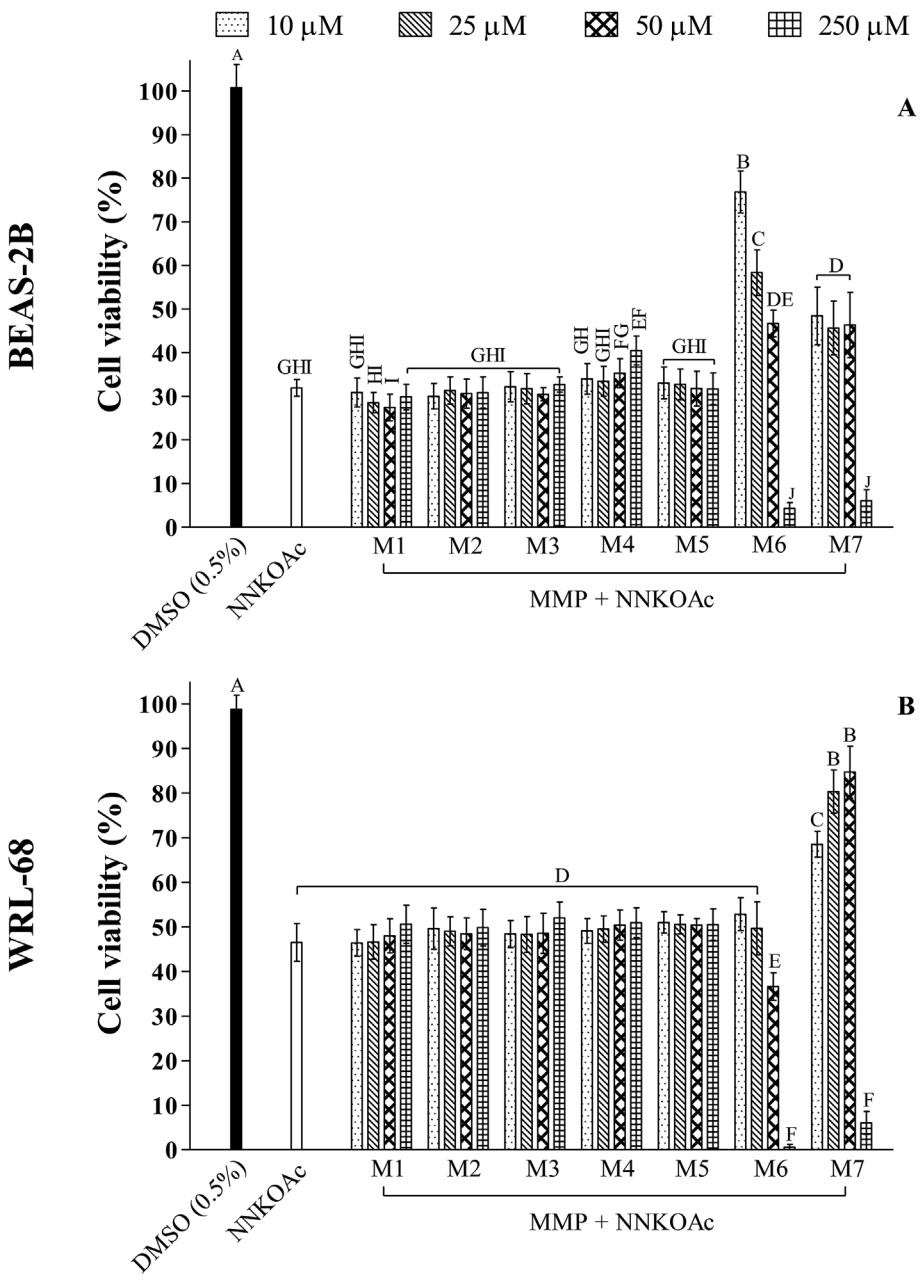

Fig. 4. Potential of microbial metabolites of proanthocyanidins (MMP) in the reduction of NNKOAc-induced cytotoxicity in BEAS-2B and WRL-68 cells. Cells were pre-exposed to MMP (10, 25, 50, and 250 µM) for 24 h and treated with NNKOAc (300 µM) for 4 h. The capacity of MMP in cytoprotection was measured as % cell viability by MTS assay. Results were presented as mean ± SD of three independent experiments. Means that do not share a similar letter are significantly different ($p \leq 0.01$). M1, 3-phenylpropionic acid; M2, 4-hydroxyphenyl acetic acid; M3, 3-(4-hydroxyphenyl) propionic acid; M4, *p*-coumaric acid; M5, benzoic acid; M6, pyrogallol; M7, pyrocatechol.

metabolism (Peterson, 2010) and successfully used in a number of studies to induce DNA damage in BEAS-2B cells. Human fetal hepatic cells (WRL-68) was used as the second cell line for this study after considering the positive relationship between tobacco smoking and liver carcinoma. NNK is a potent systemic carcinogen in tobacco smoke (Pfeifer et al., 2002), the potential in reaching the hepatocytes to induce carcinogenesis.

Tested MMP except for PG and PC showed no cytotoxicity in BEAS-2B and WRL-68 cell lines. Low cytotoxicity of simple phenolics in normal human cells is demonstrated in a number of experiments by the extremely high concentrations used to induce cytotoxicity (Galati et al., 2006). A study by Yang et al. (2009) demonstrates the PG-mediated cytotoxicity in human lung cancer cells using the MTT assay. Cytotoxicity of PG is caused by cell cycle arrest at G2 phase and induction of apoptosis (Yang et al., 2009). Furthermore, PG-treated cells are characterized by an elevated level of intracellular superoxide (Park et al., 2017). Cytotoxicity by PC is expressed as induction of apoptosis, evident by morphological disruption and DNA damage (De Oliveira et al., 2010).

It is important to consider the ability of PG and PC in the production of ROS in cell-independent culture media. Polyphenols, especially catechol, tend to experience rapid oxidation in commonly used culture media and produce H_2O_2 (Long et al., 2010). Generation of H_2O_2 in culture media leads to concentration-dependent cytotoxicity by rapid depletion of cellular ATP (Varani et al., 1990). A study by Kelts et al. (2015) demonstrated the potential of PG in the production of H_2O_2 in cell-free minimal essential media (MEM). Production of H_2O_2 in the cell culture media can affect the proliferation of cells (Lapidot et al., 2002). Therefore, the potential of PG and PC for production of H_2O_2 in cell-free BEGM and complete MEME media was evaluated by the Amplex® Red assay. Both PG and PC showed concentration-dependent production of H_2O_2 in BEGM and complete MEME media. Excessive H_2O_2 production was observed at higher concentrations (≥ 250 µM). However, the concentrations (1–50 µM) of PG and PC used for the evaluation of cyto-and genoprotective effects in this study did not produce significantly high ($p \geq 0.01$) concentrations of H_2O_2 compared to the DMSO control.

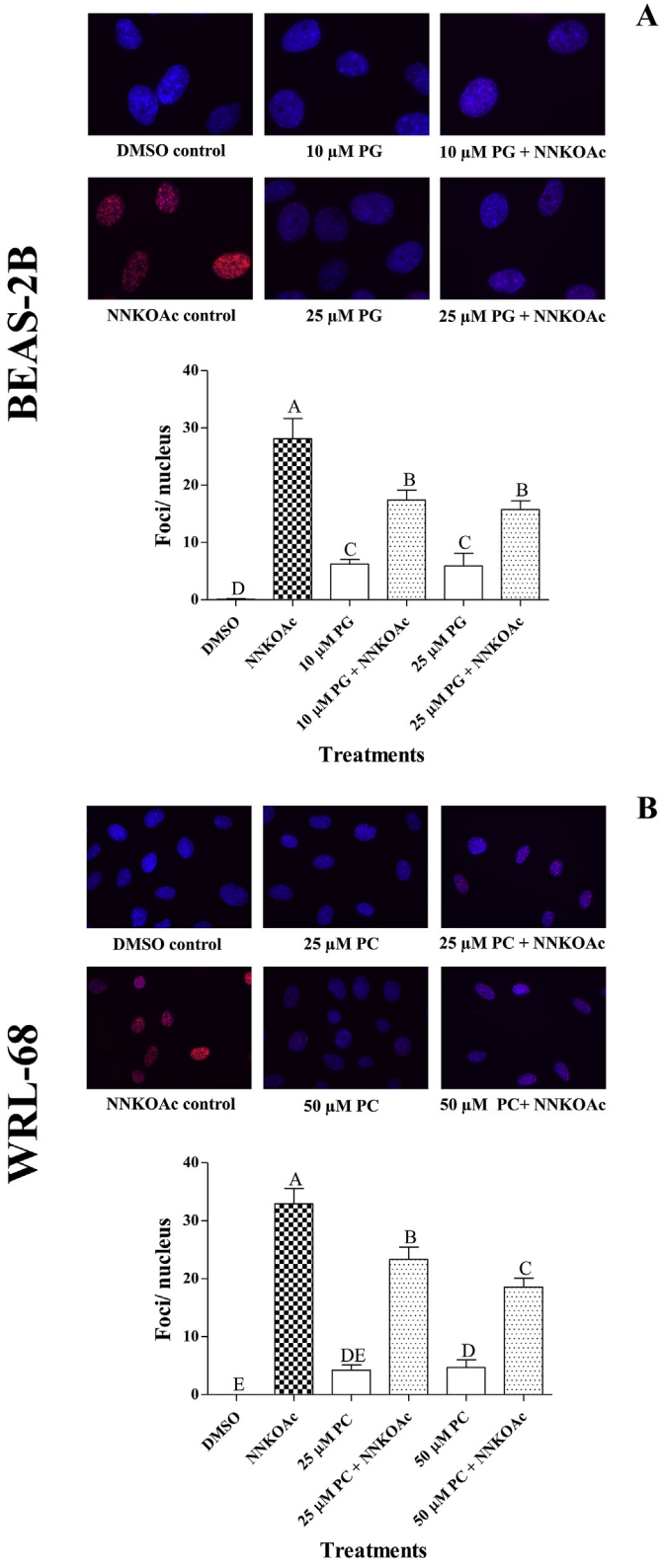

Fig. 5. Pyrogallol (PG) and pyrocatechol (PC) reduce the NNKOAC-induced DNA damage as measured by the γ-H2AX assay. BEAS-2B (A) and WRL-68 (B) cells were pre-exposed to PG and PC for 24 h, and DNA damage was induced by NNKOAc (300 μM for 4 h). Phosphorylated histone γ-H2AX foci were labeled with specific antibodies and nuclei stained with DAPI. At least 100 nuclei of each treatment were imaged by fluorescence microscopy (× 40). Number of γ-H2AX foci was counted by ImageJ software and the results averaged as foci/nucleus. Results were presented as mean ± SD of three independent experiments. Means that do not share a similar letter are significantly different ($p \leq 0.01$).

Moreover, preliminary cell viability test results on cytotoxicity of PG in BEAS-2B and PC in WRL-68 cells, showed no signs of toxicity at these concentrations, signifying the ignorable effect by H_2O_2.

Preliminary MTS test results for the investigation of MMP-mediated cytotoxicity showed promoted cell viability for PG and PC in BEAS-2B cells at lower concentrations. Augmentation of cell viability may be related with promoted cell proliferation, an undesirable effect for the mitigation of cancer occurrence. Therefore, the effect of PG and PC in cell proliferation was further studied by Oregon Green® flow cytometry assay. The proliferation of BEAS-2B cells was limited by both PG and PC in a concentration-dependent manner. Similar results were obtained for PG in WRL-68 cells. Antiproliferative activity of PG in WRL-68 cells was more prominent compared to PC. Antiproliferative properties of PG and PC are investigated in a number of cancer cell lines. A study by Yang et al. (2009) experimented with the potential of PG in limiting the proliferation of human lung cancer cells (H441 and H520). PG limits the proliferation of lung cancer cells by arresting cell cycle at G2/M phase (Yang et al., 2009). Both PG and PC type phenolics limit the cell proliferation in estrogen responsive (ER +) MCF-7 human breast cancer cells (Fernandes et al., 2010). Apart from arresting of the cell cycle at different phases, phenolics express antiproliferative properties by blocking and regulation of kinases (e.g., c-Jun *N*-terminal kinase), inhibition of transcription factors and suppression of pathways important for cell growth (Dai and Mumper, 2010). Intense antiproliferative effect of PG over PC may be possible to describe by the number of hydroxyl groups bound with the phenyl ring. Structure of PG consists of two hydroxyl groups and the PC with one hydroxyl groups bound to a single phenyl ring. Trihydroxylated phenolic acids demonstrate higher antiproliferative effect over dihydroxylated variants (Gomes et al., 2003). Thus, the high antiproliferative properties of PG over PC can be due to the higher number of hydroxyl groups.

Cytoprotection by MMP for NNKOAc-induced toxicity was investigated by MTS assay to select MMP-concentration combinations to evaluate potential in DNA damage prevention. Tested MMP except for PG and PC showed no cytoprotection in both cell lines. A study by Kling et al. (2013) investigated the cytoprotection by 19 different flavonoids, flavonoid metabolites, phenolic acid and methyl esters of phenolic acids on the neuronal cells exposed to *tert*-butyl hydroperoxide. Only the phenolics with catechol units and 4-keto group provided significant cytoprotection in the study (Kling et al., 2013). Thus, the cytoprotection by phenolics against chemical carcinogens is dependant on the functional groups available in chemical structure. The molecular structure and complexity determine the bioavailability of dietary polyphenols. PG and PC are simple phenolics detected as metabolites of colonic microbes in studies investigating the metabolism and bioavailability of dietary polyphenols. PG and PC with their methylated, sulfated, and glucuronidated metabolites are found in blood plasma and urine. Higher plasma concentrations and urinary recoveries of PG and PC together with their metabolites suggest the high bioavailability of PG and PC (Pereira-Caro et al., 2017; Feliciano et al., 2016). Moreover, PG and PC showed cell line specific activity in the reduction of NNKOAc-induced cytotoxicity. PG in BEAS-2B cells and PC in WRL-68 cells significantly reduced the cytotoxicity induced by NNKOAc. The cell line specific activity may be a result of the difference between the chemical structure of PG and PC, enzymatic systems in the two cell lines or simply the two different cell culture media. Thus, cell line specificity of PG and PC in NNKOAc-induced cytotoxicity reduction must be further investigated before declaring the specificity of PG in lung and PC in liver cancer risk reduction.

The degree of cellular DNA damage induced by NNKOAc and regulated by exposure to PG and PC was measured by γ-H2AX immunofluorescence assay. Cellular metabolism of NNK produces electrophilic metabolites capable of DNA damage (Proulx et al., 2005), characterized by the formation of bulky DNA-adducts leading to DNA double-strand breaks (DSB) generation (Hecht, 2007). The phosphorylated histone protein H2AX (γ-H2AX) is useful in the detection of DNA

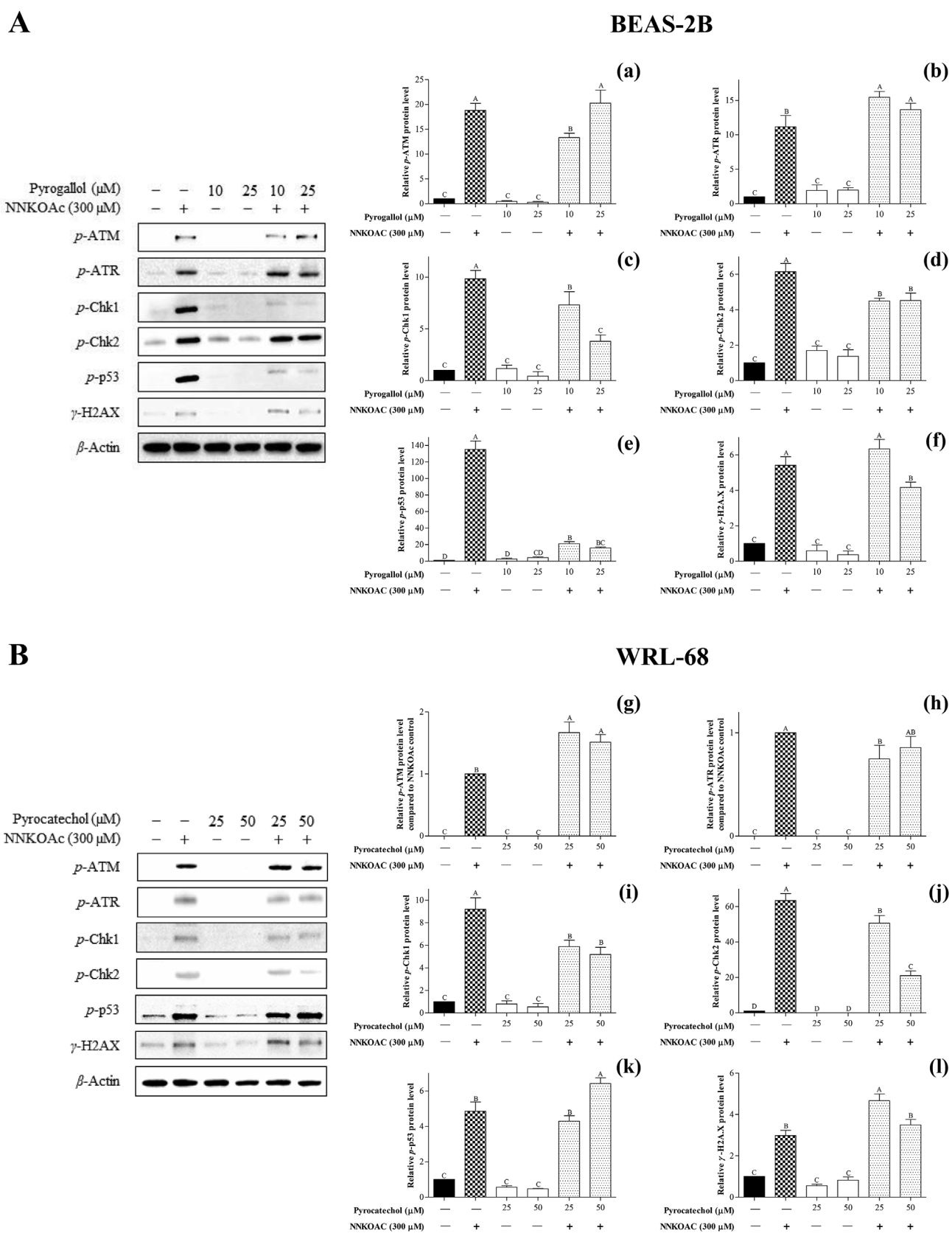

Fig. 6. Abundance of phosphorylated (*p*/γ) ATM (a, g), ATR (b, h), Chk1 (c, i), Chk2 (d, j), p53 (e, k), and H2AX (f, l) proteins in BEAS-2B (A) and WRL-68 (B) cells. BEAS-2B cells were treated with 10 and 25 μM of pyrogallol (A) and WRL-68 cells were treated with 25 and 50 μM of pyrocatechol (B) before exposed to 300 μM NNKOAc for 4 h. The level of expression of DNA damage repair proteins were quantified by western blotting. Results were expressed as relative protein levels compared to the DMSO control. At least three western blotting experiments were performed, and the results were expressed with means ± standard deviations. Results were statistically analyzed by one-way ANOVA and Tukey's mean separation (α = 0.01) using Minitab statistical software.

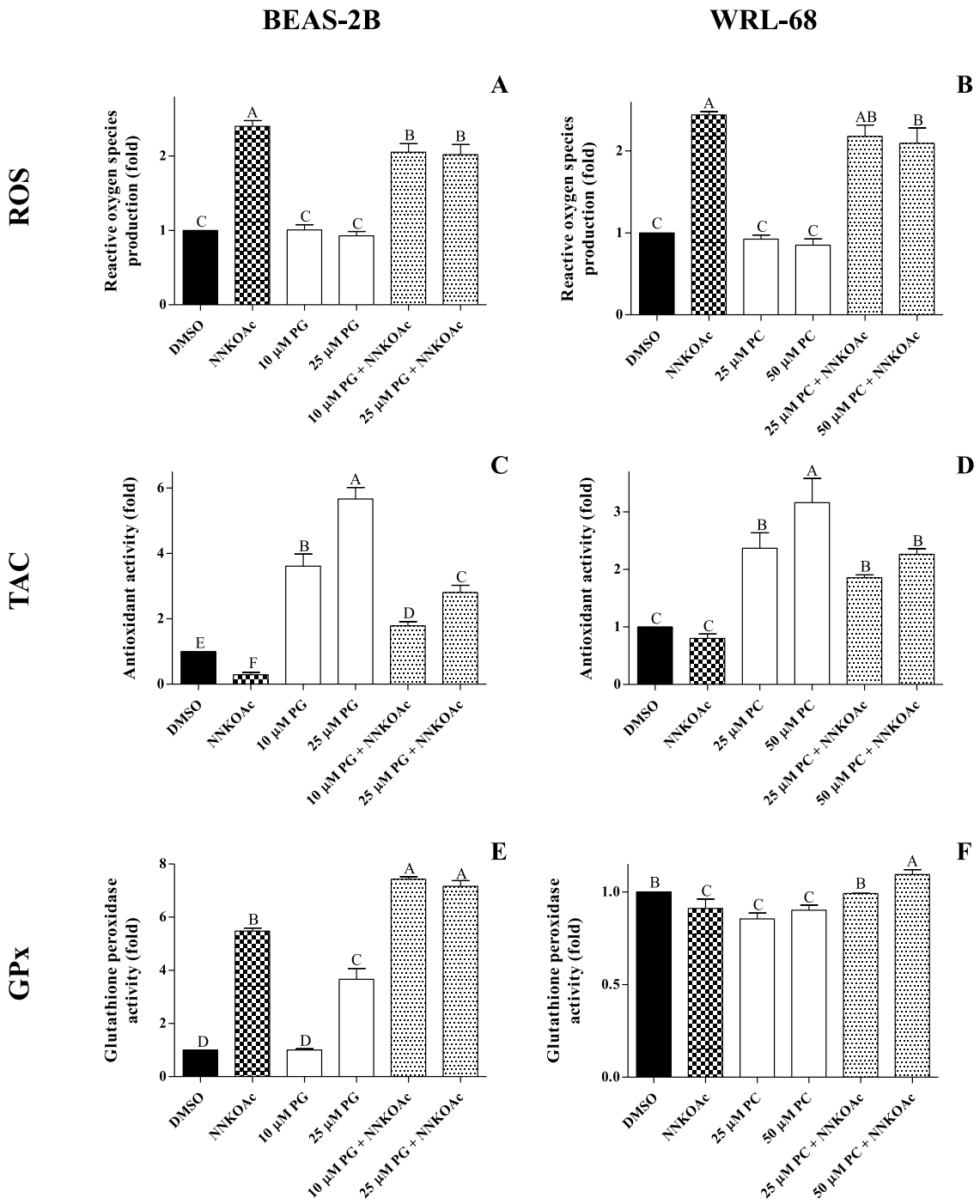

Fig. 7. The potential of pyrogallol (PG) and pyrocatechol (PC) in alleviating NNKOAc-induced oxidative stress in BEAS-2B and WRL-68 cells. BEAS-2B and WRL-68 cells were pre-treated with PG (10 and 25 µM) and PC (25 and 50 µM), respectively for 24 h. The cells were exposed to NNKOAc (300 µM for 4 h) to induce oxidative stress and the cellular reactive oxygen species (ROS) level, total antioxidant capacity (TAC), and glutathione peroxidase (GPx) activity were measured. Results were presented as mean ± SD of three independent experiments. Means that do not share a similar letter are significantly different ($p \leq 0.01$).

damage at the histone protein level, particularly the DSB (Zhou et al., 2006). Cellular DNA damage protection by PG in BEAS-2B cells and PC in WRL-68 cells was evaluated considering their performance in cyto-protection against NNKOAc. The γ-H2AX test results showed that both PG and PC could protect the cells from NNKOAc-induced DNA damage (Fig. 5). The PG and PC treatment alone showed an increment in cellular DNA damage compared to the DMSO control. PG and PC may have induced DNA strand break through induction of topoisomerase (1 and 2)-DNA complexes. Induction of topoisomerase-DNA complexes by PG and PC may have resulted by their potential to generate H_2O_2 by autoxidation (Lopez-Lazaro et al., 2011). However, the concentrations of PG (10 and 25 µM) and PC (25 and 50 µM) used in cytotoxicity and DNA damage reduction analysis showed no significant production of H_2O_2 in the cell culture media (as shown by Amplex® Red assay). We further investigated the potential of PG and PC in NNKOAc-induced DNA damage reduction by using the comet assay, also called single-cell gel electrophoresis (Supplementary Fig. 2). As a result of DNA damage to strands, DNA supercoiled structure relaxes and enables anode directed DNA migration in gel electrophoresis. The intensity of damage resembles a comet under fluorescence microscopy and can be evaluated

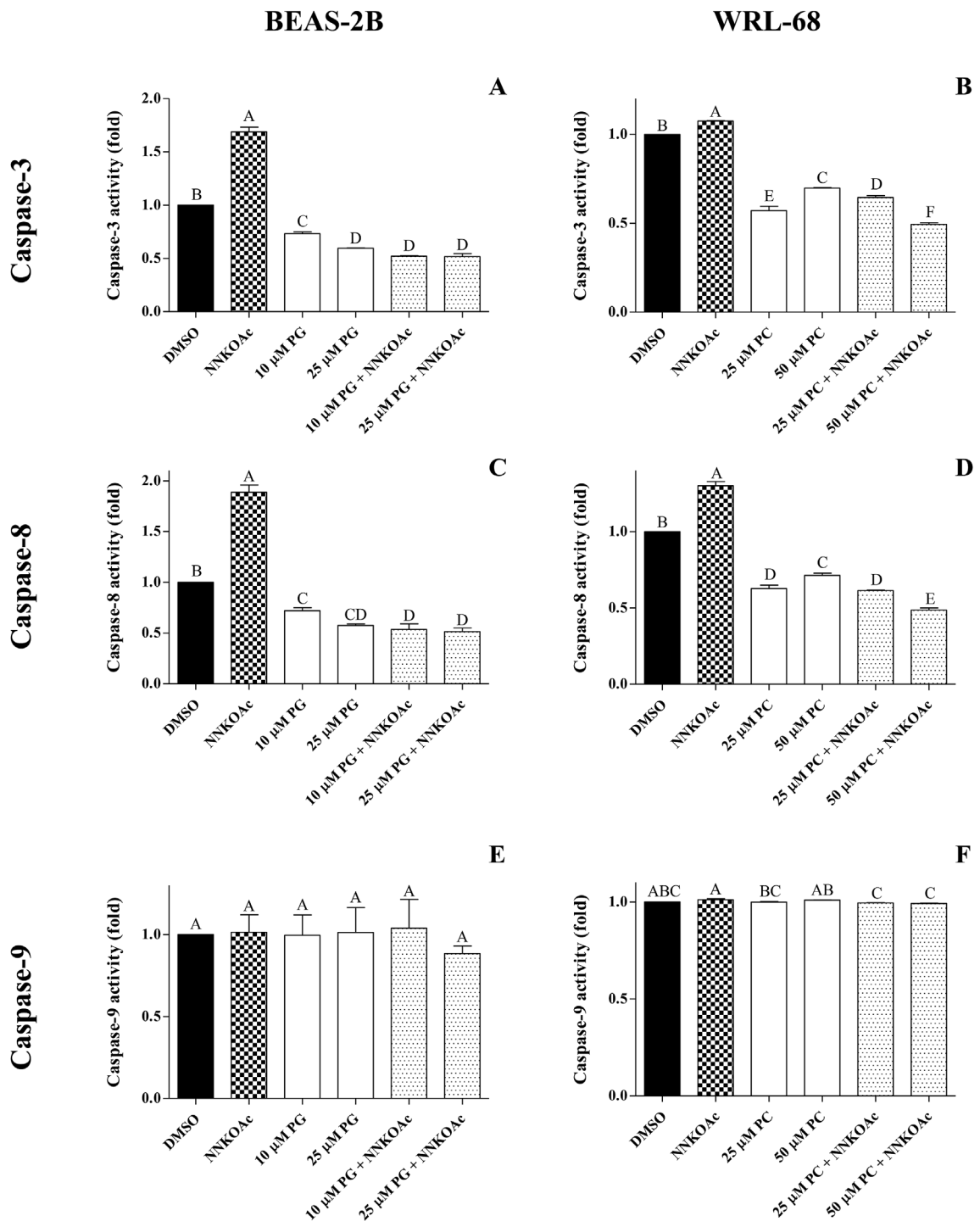

Fig. 8. Effect of pyrogallol (PG) and pyrocatechol (PC) on NNKOAc-induced apoptosis in BEAS-2B and WRL-68 cells. BEAS-2B and WRL-68 cells were pre-treated with PG (10 and 25 μM) and PC (25 and 50 μM), respectively for 24 h. The cells were exposed to NNKOAc (300 μM for 4 h) to induce apoptosis cascade. The enzyme activity of caspase-3, 8, and 9 were measured. Results were presented as mean ± SD of three independent experiments. Means that do not share a similar letter are significantly different ($p \leq 0.01$).

by using OpenComet™ computer software (http://www.cometbio.org). The results were expressed as Olive tail moment which is the product of comet tail DNA% and the distance between the comet head and tail centroids (Gyori et al., 2014). Cells pre-treated with PG and PC depicted low mean DNA damages (Olive tail moments) compared to the NNKOAc control supporting the γ-H2AX test results. However, statistical significance could not be observed due to the high variation of Olive tail moments.

Anticancer properties of phenolics are also demonstrated by complex interventions with metabolic pathways and gene modulation (George et al., 2017). Therefore, we studied the influence of PG and PC treatment on the key proteins of DDR mechanisms by western blot analysis. Activation/phosphorylation of ATM, ATR, Chk1, Chk2, p53, and histone protein H2AX is common in cells experiencing DNA damage and replication stress (Yan et al., 2014). These proteins are capable in the modulation of cellular DDR mechanisms for cell proliferation, cell cycle arrest and apoptosis (George et al., 2017). ATM and ATR are the key regulatory proteins of DDR mechanisms. Activation of ATM

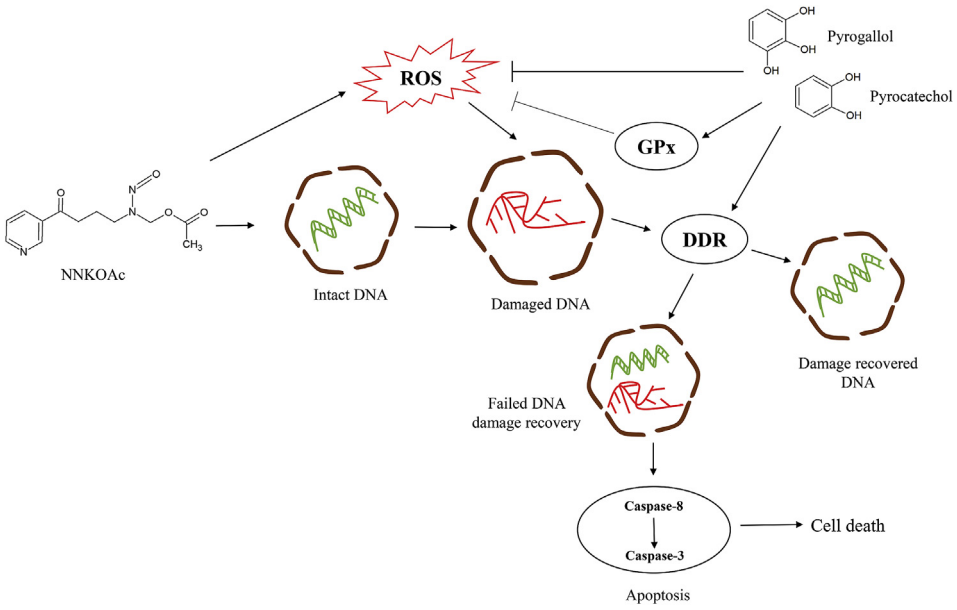

Fig. 9. Pyrogallol (PG) in BEAS-2B cells and pyrocatechol (PC) in WRL-68 cells reduce NNKOAc-induced DNA damage. NNKOAc induces cellular DNA damage by bulky adduct formation and reactive oxygen species (ROS) production. PG and PC act as antioxidants and promote cellular enzymatic antioxidant GPx to reduce DNA damage by ROS neutralization. Damaged DNA triggers cellular DNA damage response (DDR) mechanism to maintain genomic integrity. PG and PC influence DDR by altering the expression of DDR proteins (ATM, ATR, Chk1, Chk2, p53, and H2AX). Failure to overcome DNA damage initiates programmed cell death (apoptosis) by triggering caspase cascade. PG and PC suppress the extrinsic apoptotic pathway by limiting caspase-3 and 8 expressions.

and ATR is dependent on the nature of DNA damage, and the functionality of the two kinases is distinct from each other. ATM activation predominantly results in DNA DSB while ATR activation occurs through a number of DNA damages including bulky lesions by methylation (Marechal and Zou, 2013). Repair of DNA DSB through ATR activation is achieved through the conversion of DSB into single-strand DNA (ssDNA) by resection with the help of ATM (Marechal and Zou, 2013). ATM-Chk2 checkpoint activation and ATR-Chk1 checkpoint activation are two important pathways in DDR (Yan et al., 2014). BEAS-2B and WRL-68 cells exposed to NNKOAc showed substantial upregulation of targeted DDR proteins, ensuring the activation of DDR pathways. Treatment with PG affected the ATR-Chk1 pathway by significantly upregulating *p*-ATR and downregulating (concentration-dependant) *p*-Chk1 in BEAS-2B cells exposed to NNKOAc. DNA damage by NNKOAc causes the formation of bulky DNA lesions and adducts. Bulky DNA lesions is a major drive for ATR activation. Further experimentation for the detection of other proteins activated or inactivated by ATR (e.g., Cdk1) is recommended to establish a clear connection between PG treatment and the effect on the ATR-Chk1 pathway. PG also influenced the ATM-Chk2 checkpoint pathway in NNKOAc exposed BEAS-2B cells by downregulation of *p*-ATM, *p*-Chk2, *p*-p53, and γ-H2AX expression. George and Rupasinghe (2017) reported similar results (except upregulation of *p*-ATR) for BEAS-2B cells treated with flavonoids and challenged for genotoxicity by NNKOAc. Furthermore, the study suggests the potential of flavonoids in promoting ATR-dependant DNA damage reduction. In contrast to PG in NNKOAc-treated BEAS-2B cells, PC upregulated the expression of *p*-ATM and restricted *p*-ATR expression in WRL-68 cells exposed to NNKOAc. PC-mediated downregulation of *p*-Chk2 in NNKOAc exposed WRL-68 cells was concentration-dependant. Upregulated expression of *p*-p53 and γ-H2AX suggests the activation of the ATM-Chk2 pathway in NNKOAc exposed WRL-68 cells. Furthermore, the influence of the PC on the ATR-Chk1 pathway is demonstrated by the downregulation of *p*-ATR and *p*-Chk1. However, the results remain inconclusive and recommend further experimentation to identify prominent DDR mechanisms.

The ability of polyphenols in DNA damage reduction by acting as antioxidant agents is appreciated by many researchers using a number of polyphenols with chemical and metallic carcinogens (George and Rupasinghe, 2017; Gill et al., 2010; Thilakarathna et al., 2018). Cytoprotective and genoprotective properties of PG and PC may be contributed by their antioxidant activity. Antioxidant activities of PG and PC are well documented (Sarikaya, 2015; Kosobutskii, 2014). PG in BEAS-2B cells and PC in WRL-68 cells improved the TAC of cells and suppressed the ROS levels elevated by NNKOAc. Cells are equipped with various antioxidants and enzymatic antioxidant systems to reduce cellular oxidative stress. GPx, superoxide dismutase (SOD), catalase are the major enzymatic antioxidants active (radical scavengers) in lungs. GPx mitigates the cellular oxidative stress by reducing H_2O_2 into H_2O (Birben et al., 2012). PG and PC significantly increased the expression of enzymatic antioxidant GPx in cells exposed to NNKOAc. Thus, the ROS reduction in NNKOAc exposed cells can be contributed by the PG and PC-mediated GPx (enzymatic antioxidant) promotion. However, the GPx expression of WRL-68 cells was limited upon the treatment with PC independent of NNKOAc. Similar results are reported for male Swiss albino mice (liver) administered with 40 mg/kg body weight of PG (Upadhyay et al., 2007).

Cellular DNA damage can lead to the cascade of apoptotic events when DDR mechanisms fail to maintain genome integrity. DNA methylation and formation of bulky DNA adducts are two major DNA lesions initiating cell apoptosis (Roos and Kaina, 2013). Cell death can occur through either of three apoptotic pathways: caspase-dependent extrinsic and intrinsic or caspase-independent pathways. We studied the expression of key effectors for the extrinsic pathway (caspase-8), and intrinsic pathway (caspase-9) and central effector (caspase-3) for both pathways. Exposure of cells to NNKOAc elevated the expression of caspase-3 and 8, suggesting the activation of the extrinsic apoptotic pathway by this carcinogen. Suppression of NNKOAc-induced caspase-3 and 8 expressions by treatment with PG and PC explains their potential to protect the cells from cyto- and genotoxicity of NNKOAc. However, further experimentation is required to understand whether the suppression of caspase-activity is truly beneficial, as apoptosis plays an important role by the elimination of cancerous cells.

5. Conclusion

Tested MMP except for PG and PC at high concentrations are not cytotoxic in BEAS-2B and WRL-68 cells. Cytotoxicity triggered by PG and PC is due to the concentration-dependent H_2O_2 production in cell culture media. The promoted % cell viability in BEAS-2B cells by lower concentrations of PG and PC is not characterized by induced cell proliferation. Cytoprotection by MMP against NNKOAc is cell line specific, and only PG and PC protected the BEAS-2B and WRL-68 cells, respectively. PG in BEAS-2B cells and PC in WRL-68 cells reduce the DNA damage induced by NNKOAc. PG and PC may contribute to the

reduction of cellular DNA damage by altering the expression of DDR protein and suppressing NNKOAc-induced oxidative stress by promoting TAC and GPx activity. PG in BEAS-2B cells and PC in WRL-68 cells can suppress the expression of the extrinsic apoptotic pathway (caspase 8–3) provoked by NNKOAc. This study shows the potential of MMP to mitigate cancer risk by altering the DDR protein expression and promoting cellular antioxidant defense. Further experimentation using animal models can be recommended to illustrate the importance of intestinal microbiome in the biotransformation of PAC into simple metabolites for cancer risk reduction.

Authors' contributions

WPDWT performed all the experiments, analyzed the data and drafted the manuscript. HPVR, the principal investigator, designed the study and made intellectual contributions to the manuscript. Both authors have read and approved the final manuscript.

Conflicts of interest

The authors declare that there is no conflict of interest.

Acknowledgments

This study was supported by the Discovery Grant of Natural Sciences and Engineering Research Council of Canada (HPVR) and the Cancer Research Training Program of the Beatrice Hunter Cancer Research Institute supported by the Saunders-Matthey cancer prevention foundation (WPDWT).

Appendix A. Supplementary data

Supplementary data to this article can be found online at https://doi.org/10.1016/j.fct.2019.02.010.

Transparency document

Transparency document related to this article can be found online at https://doi.org/10.1016/j.fct.2019.02.010.

References

Akinmoladun, A.C., Ibukun, E.O., Afor, E., Obuotor, E.M., Farombi, E.O., 2007. Phytochemical constituent and antioxidant activity of extract from the leaves of *Ocimum gratissimum*. Sci. Res. Essays 2 (5), 163–166.

Birben, E., Sahiner, U.M., Sackesen, C., Erzurum, S., Kalayci, O., 2012. Oxidative stress and antioxidant defense. World Allergy Org. J. 5 (1), 9–19.

Cadet, J., Wagner, J.R., 2013. DNA base damage by reactive oxygen species, oxidizing agents, and UV radiation. Cold Spring Harbor Perspect. Biol. 5, a012559 2013.

Dai, J., Mumper, R.J., 2010. Plant phenolics: extraction, analysis and their antioxidant and anticancer properties. Molecules 15 (10), 7313–7352.

De Oliveira, D.M., Pitanga, B.P.S., Grangeiro, M.S., Lima, R.M.F., Costa, M.D.F.D., Costa, S.L., Clarencio, J., El-Bacha, R.D.S., 2010. Catechol cytotoxicity in vitro: induction of glioblastoma cell death by apoptosis. Hum. Exp. Toxicol. 29 (3), 199–212.

Demizu, Y., Sasaki, R., Trachootham, D., Pelicano, H., Colacino, J.A., Liu, J., Huang, P., 2008. Alterations of cellular redox state during NNK-induced malignant transformation and resistance to radiation. Antioxidants Redox Signal. 10 (5), 951–962.

Deprez, S., Brezillon, C., Rabot, S., Philippe, C., Mila, I., Lapierre, C., Scalbert, A., 2000. Polymeric proanthocyanidins are catabolized by human colonic microflora into low-molecular-weight phenolic acids. J. Nutr. 130 (11), 2733–2738.

Feliciano, R.P., Boeres, A., Massacessi, L., Istas, G., Ventura, M.R., dos Santos, C.N., Heiss, C., Rodriguez-Mateos, A., 2016. Identification and quantification of novel cranberry-derived plasma and urinary (poly) phenols. Arch. Biochem. Biophys. 599, 31–41.

Fernandes, I., Faria, A., Azevedo, J., Soares, S., Calhau, C., De Freitas, V., Mateus, N., 2010. Influence of anthocyanins, derivative pigments and other catechol and pyrogallol-type phenolics on breast cancer cell proliferation. J. Agric. Food Chem. 58 (6), 3785–3792.

Galati, G., Lin, A., Sultan, A.M., O'brien, P.J., 2006. Cellular and in vivo hepatotoxicity caused by green tea phenolic acids and catechins. Free Radic. Biol. Med. 40 (4), 570–580.

Garcia-Canton, C., Minet, E., Anadon, A., Meredith, C., 2013. Metabolic characterization of cell systems used in *in vitro* toxicology testing: lung cell system BEAS-2B as a working example. Toxicol. Vitro 27, 1719–1727.

George, V.C., Rupasinghe, H.P.V., 2017. Apple flavonoids suppress carcinogens-induced DNA damage in normal human bronchial epithelial cells. Oxidative Med. Cell. Longev. 2017, 1767198 12 pages.

George, V.C., Dellaire, G., Rupasinghe, H.V., 2017. Plant flavonoids in cancer chemoprevention: role in genome stability. J. Nutr. Biochem. 45, 1–14.

Gill, C.I., Hashim, Y.Z.H.Y., Servili, M., Rowland, I.R., 2010. Olive oil and its phenolic components and their effects on early-and late-stage events in Carcinogenesis. In: Olives and Olive Oil in Health and Disease Prevention, pp. 1005–1012.

Gomes, C.A., Girao da Cruz, T., Andrade, J.L., Milhazes, N., Borges, F., Marques, M.P.M., 2003. Anticancer activity of phenolic acids of natural or synthetic origin: a structure-activity study. J. Med. Chem. 46 (25), 5395–5401.

Gyori, B.M., Venkatachalam, G., Thiagarajan, P.S., Hsu, D., Clement, M.V., 2014. OpenComet: an automated tool for comet assay image analysis. Redox Biol. 2, 457–465.

Hecht, S.S., 2007. Progress and challenges in selected areas of tobacco carcinogenesis. Chem. Res. Toxicol. 21 (1), 160–171.

Ivashkevich, A., Redon, C.E., Nakamura, A.J., Martin, R.F., Martin, O.A., 2012. Use of the γ-H2AX assay to monitor DNA damage and repair in translational cancer research. Cancer Lett. 327 (1–2), 123–133.

Jia, P., Her, C., Chai, W., 2015. DNA excision repair at telomeres. DNA Repair 36, 137–145.

Kelts, J.L., Cali, J.J., Duellman, S.J., Shultz, J., 2015. Altered cytotoxicity of ROS-inducing compounds by sodium pyruvate in cell culture medium depends on the location of ROS generation. SpringerPlus 4 (1), 269.

Kling, B., Bücherl, D., Palatzky, P., Matysik, F.M., Decker, M., Wegener, J., Heilmann, J., 2013. Flavonoids, flavonoid metabolites, and phenolic acids inhibit oxidative stress in the neuronal cell line HT-22 monitored by ECIS and MTT assay: a comparative study. J. Nat. Prod. 77 (3), 446–454.

Kosobutskii, V.S., 2014. Pyrocatechol and its derivatives as antioxidants and prooxidants. Russ. J. Gen. Chem. 84 (5), 839–842.

Lapidot, T., Walker, M.D., Kanner, J., 2002. Can apple antioxidants inhibit tumor cell proliferation? Generation of H2O2 during interaction of phenolic compounds with cell culture media. J. Agric. Food Chem. 50 (11), 3156–3160.

Li, S., Chen, L., Yang, T., Wu, Q., Lv, Z., Xie, B., Sun, Z., 2013. Increasing antioxidant activity of procyanidin extracts from the pericarp of *Litchi chinensis* processing waste by two probiotic bacteria bioconversions. J. Agric. Food Chem. 61 (10), 2506–2512.

Long, L.H., Hoi, A., Halliwell, B., 2010. Instability of, and generation of hydrogen peroxide by, phenolic compounds in cell culture media. Arch. Biochem. Biophys. 501 (1), 162–169.

Lopez-Lazaro, M., Calderón-Montano, J.M., Burgos-Moron, E., Austin, C.A., 2011. Green tea constituents (−)-epigallocatechin-3-gallate (EGCG) and gallic acid induce topoisomerase I–and topoisomerase II–DNA complexes in cells mediated by pyrogallol-induced hydrogen peroxide. Mutagenesis 26 (4), 489–498.

Marechal, A., Zou, L., 2013. DNA damage sensing by the ATM and ATR kinases. Cold Spring Harbor Perspect. Biol. 5, a012716.

Molina, J.R., Yang, P., Cassivi, S.D., Schild, S.E., Adjei, A.A., 2008. Non-small cell lung cancer: epidemiology, risk factors, treatment, and survivorship. Mayo Clin. Proc. 83 (5), 584–594.

Nowsheen, S., Yang, E.S., 2012. The intersection between DNA damage response and cell death pathways. Exp. Oncol. 34 (3), 243–254.

Ou, K., Gu, L., 2014. Absorption and metabolism of proanthocyanidins. J. Funct. Foods 7, 43–53.

Pang, Q., Qu, K., Zhang, J., Xu, X., Liu, S., Song, S., Wang, R., Zhang, L., Wang, Z., Liu, C., 2015. Cigarette smoking increases the risk of mortality from liver cancer: a clinical-based cohort and meta-analysis. J. Gastroenterol. Hepatol. 30 (2015), 1450–1460.

Park, H.J., Choi, Y.J., Lee, J.H., Nam, M.J., 2017. Naringenin causes ASK1-induced apoptosis via reactive oxygen species in human pancreatic cancer cells. Food Chem. Toxicol. 99, 1–8.

Parmar, I., Rupasinghe, H.P.V., 2014. Proanthocyanidins in cranberry and grape seeds: metabolism, bioavailability, and biological properties. In: Brar, S.K., Kaur, S., Dhillon, G.S. (Eds.), Nutraceuticals and Functional Foods: Natural Remedy. Nova Science Publishers, Inc., New York, pp. 119–145.

Pereira-Caro, G., Moreno-Rojas, J.M., Brindani, N., Del Rio, D., Lean, M.E., Hara, Y., Crozier, A., 2017. Bioavailability of black tea theaflavins: absorption, metabolism, and colonic catabolism. J. Agric. Food Chem. 65 (26), 5365–5374.

Peterson, L.A., 2010. Formation, repair, and genotoxic properties of bulky DNA adducts formed from tobacco-specific nitrosamines. J. Nucleic Acids 2010. https://doi.org/10.4061/2010/284935.

Pfeifer, G.P., Denissenko, M.F., Olivier, M., Tretyakova, N., Hecht, S.S., Hainaut, P., 2002. Tobacco smoke carcinogens, DNA damage and p53 mutations in smoking-associated cancers. Oncogene 21 (48), 7435–7451.

Proulx, L.I., Gaudreault, M., Turmel, V., Augusto, L.A., Castonguay, A., Bissonnette, E.Y., 2005. 4-(Methylnitrosamino)-1-(3-pyridyl)-1-butanone, a component of tobacco smoke, modulates mediator release from human bronchial and alveolar epithelial cells. Clin. Exp. Immunol. 140 (1), 46–53.

Roos, W.P., Kaina, B., 2013. DNA damage-induced cell death: from specific DNA lesions to the DNA damage response and apoptosis. Cancer Lett. 332 (2), 237–248.

Rupasinghe, H.P.V., Thilakarathna, S., Nair, S., 2013. Polyphenols of apples and their potential health benefits. In: Sun, J., Prasad, K.N., Ismail, A. (Eds.), Polyphenols: Chemistry, Dietary Sources and Health Benefits. Nova Science Publishers, Inc., New York, pp. 333–368.

Sarikaya, S.B.O., 2015. Acetylcholinesterase inhibitory potential and antioxidant properties of pyrogallol. J. Enzym. Inhib. Med. Chem. 30 (5), 61–766.

Schneider, C.A., Rasband, W.S., Eliceiri, K.W., 2012. NIH Image to ImageJ: 25 years of image analysis. Nat. Methods 9 (7), 671–675.

Shen, Z., 2011. Genomic instability and cancer: an introduction. J. Mol. Cell Biol. 3, 1–3.
Si, W., Gong, J., Tsao, R., Kalab, M., Yang, R., Yin, Y., 2006. Bioassay-guided purification and identification of antimicrobial components in Chinese green tea extract. J. Chromatogr. A 1125, 204–210.
Siegel, R.L., Miller, K.D., Jemal, A., 2017. Cancer statistics, 2017. CA A Cancer J. Clin. 67, 7–30.
Sun, L., Liu, Y.M., Chen, B.Q., Liu, Q.H., 2015. New phenolic compounds from the seeds of *Nigella glandulifera* and their inhibitory activities against human cancer cells. Bioorg. Med. Chem. Lett 25 (18), 3864–3866.
Tabasco, R., Sanchez-Patan, F., Monagas, M., Bartolome, B., Moreno-Arribas, M.V., Pelaez, C., Requena, T., 2011. Effect of grape polyphenols on lactic acid bacteria and bifidobacteria growth: resistance and metabolism. Food Microbiol. 28 (7), 1345–1352.
Thilakarathna, S., Rupasinghe, H.P.V., 2013. Flavonoid bioavailability and attempts for bioavailability enhancement. Nutrients 5, 3367–3387.
Thilakarathna, W.P.D.W., Langille, M., Rupasinghe, H.P.V., 2018. Polyphenol-based prebiotics and synbiotics: potential for cancer chemoprevention. Curr. Opin. Food Sci. 20, 51–57.
Tsao, R., 2010. Chemistry and biochemistry of dietary polyphenols. Nutrients 2, 1231–1246.
Upadhyay, G., Kumar, A., Singh, M.P., 2007. Effect of silymarin on pyrogallol-and rifampicin-induced hepatotoxicity in mouse. Eur. J. Pharmacol. 565 (1–3), 190–201.
Varani, J., Phan, S.H., Gibbs, D.F., Ryan, U.S., Ward, P.A., 1990. H_2O_2-mediated cytotoxicity of rat pulmonary endothelial cells. Changes in adenosine triphosphate and purine products and effects of protective interventions. Lab. Invest. 63 (5), 683–689.
Vuong, Q.V., Hirun, S., Phillips, P.A., Chuen, T.L.K., Bowyer, M.C., Goldsmith, C.D., Scarlett, C.J., 2014. Fruit-derived phenolic compounds and pancreatic cancer: perspectives from Australian native fruits. J. Ethnopharmacol. 152 (2), 227–242.
Yan, S., Sorrell, M., Berman, Z., 2014. Functional interplay between ATM/ATR-mediated DNA damage response and DNA repair pathways in oxidative stress. Cell. Mol. Life Sci. 71 (20), 3951–3967.
Yang, C.J., Wang, C.S., Hung, J.Y., Huang, H.W., Chia, Y.C., Wang, P.H., Weng, C.F., Huang, M.S., 2009. Pyrogallol induces G2-M arrest in human lung cancer cells and inhibits tumor growth in an animal model. Lung Canc. 66 (2), 162–168.
Zhou, C., Li, Z., Diao, H., Yu, Y., Zhu, W., Dai, Y., Chen, F.F., Yang, J., 2006. DNA damage evaluated by γ-H2AX foci formation by a selective group of chemical/physical stressors. Mutat. Res. Genet. Toxicol. Environ. Mutagen 604 (1), 8–18.